

# Optimization of Layout and Path Planning of Surgical Robotic System

Quoc Cuong Nguyen, Youngjun Kim, and HyukDong Kwon\*

**Abstract:** Positioning a surgical robot for optimal operation in a crowded operating room is a challenging task. In the robotic-assisted surgical procedures, the surgical robot's end-effector must reach the patient's anatomical targets because repositioning of the patient or surgical robot requires additional time and labor. This paper proposes an optimization algorithm to determine the best layout of the operating room, combined with kinematics criteria and optical constraints applied to the surgical assistant robot system. A new method is also developed for trajectory of robot's end-effector for path planning of the robot motion. The average deviations obtained from repeatability tests for surgical robot's layout optimization were 1.4 and 4.2 mm for x and y coordinates, respectively. The results of this study show that the proposed optimization method successfully solves the placement problem and path planning of surgical robotic system in operating room.

**Keywords:** Genetic algorithm, medical robot, operating room layout, optimization, path planning.

## 1. INTRODUCTION

The environment in the operating room (OR) is crowded, with many medical instruments, including the robot, surrounding the patient. Fig. 1 illustrates the layout of an OR with a surgical assistant robot system.

A suitable layout is required that encompasses the medical robotic system to avoid any possible collision between the robot and surrounding objects for enhancing patient safety. Moreover, if the surgical robot or navigation camera requires repositioning so that it can reach the planned target or track the target objects, the setup time will increase. An optimization algorithm is necessary to solve these problems and create an optimal layout in the OR.

The aim of optimizing the position of the surgical assistant robot and navigation camera in the OR is to decrease the preparation time required for robot-assisted surgery by avoiding repositioning the surgical robot and/or navigation camera. For industrial robots, several methods have been proposed to optimize the robot positioning considering various constraint criteria. Correa and Dutra [1] proposed a method to locate the manipulator by using energy calculation and heuristic search. Kamrani *et al.* [2] optimized the placement of prescribed task of a manipulator by using response surface method on concept of path translation and path rotation. Malek and Yu [3] introduced a search method to optimize the placement of a serial robot manipulator by using the genetic algorithm. They

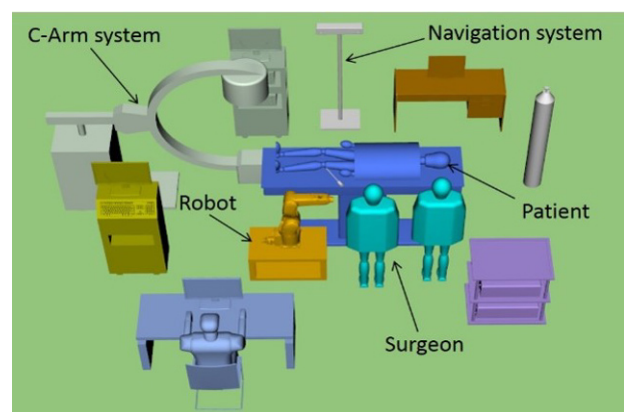


Fig. 1. 3D model of operation room layout with medical instruments, surgical robot and the patient.

used a mathematical model to obtain the workspace envelope in terms of closed-form equations of surface patches. In their research, however, the robot workspace was only constructed by the target point's position, excluding the point's orientation. Similarly, He *et al.* [4] presented an optimal placement method using the genetic algorithm for automatic location of the manipulator mounted on a multi-freedom crossbeam in order to optimize multiple kinematics during the execution of a task. Tian and Collins [5] also introduced the optimal placement of the manipulator by using the genetic algorithm.

Manuscript received November 10, 2015; revised March 26, 2016; accepted May 18, 2016. Recommended by Associate Editor Huaping Liu under the direction of Editor Fuchun Sun. This work was supported by the KIST institutional program (2E26210, 2E26276).

Quoc Cuong Nguyen and Hyukdong Kwon are with the Graduate School of NID Fusion Technology, Seoul National University of Science and Technology, 232 Gongneung-ro, Nowon-gu, Seoul 01811, Korea (e-mails: {nqcuong, atom}@seoultech.ac.kr). Youngjun Kim is with the Center for Bionics, Korea Institute of Science and Technology, 5 Hwarang-ro 14 gil, Seongbuk-gu, Seoul 02792, Korea (e-mail: junekim@kist.re.kr).

\* Corresponding author.

However, their research was only applied to a problem with a small number of degrees of freedom. Therefore, their method cannot be used in the application of space tasks. Misti *et al.* [6] presented an optimal algorithm for locating the base position of a spatial robot when the end-effector poses are prescribed to avoid singular configurations. The placement of robotic milling was presented by G.C Vosniakos and E. Matsas [7] to select the most suitable initial pose of the robot for placement with respect to workpiece. A numerical formulation for placement of open-loop robot manipulators in an environment with aim of reaching specific target points was introduced by Yang *et al.* [8]. Trabia and Kathari [9] investigated the base placement of a robot for minimum path traversal time for an end-effector of a serially connected robotic manipulator. Simultaneous analysis of both manipulability and mechanical power based on optimal task placement for a serial manipulator was presented by Santos *et al.* [10].

Although many approaches have been proposed to solve the optimization problems of factory layout, only a few optimization approaches can be found for surgical robot system in OR. Because the issues pertaining to surgical environment including surgical time and patient safety are more critical than the problems in industrial robot, it is imperative to investigate the optimization of surgical robot systems. For surgical assistant robots, Adhami *et al.* [11, 12] proposed a systematic method for the positioning surgical robots with a high number of degrees of freedom for optimal operation. Maniere *et al.* [13] developed a two-step strategy to optimize the most critical setting of a robotically assisted, minimally invasive surgery. For camera placement, J.G.Barbosa *et al.* [14] presented camera placement for total coverage by using surface-project workspace and camera projection model. An algorithm for optimal camera placement considering camera specification was presented by K. Yabuta and H. Kitazawa [15]. E. Yildiz *et al.* [16] proposed a-level algorithm to find the optimal camera placement for providing angular coverage in Wireless Video Sensor Networks. However, these approaches have limitations regarding practicability and application scope. These studies mainly focus on the prevention of collisions between multiple manipulators of a surgical robot without considering robot positioning. Optimal robot positioning is important to maximize manipulability, which is required to reach all surgical targets without repositioning. If the surgical robot's manipulability is maximized, the robot end-effector can reach all the targets regardless of patient movement.

For path planning, many research groups have addressed mostly for industrial robots, and a few approaches have been proposed in surgical robots. Path planning is an essential procedure to control the robot end-effector's moving path. During surgery, path of the end-effector of the surgical robot should be optimally planned avoiding

collision with patient and other instruments. Path planning should be also updated in real time according the patient movement. R. Ye and Y. Chen [17] proposed an automatic reduction path planning based on the shortest linear for fracture reduction surgery. J. Zhang *et al.* [18] presented an optimal path planning method of steerable electrode arrays for robot-assisted cochlear surgery. To optimize the path planning, the shape discrepancies of the bent electrode array throughout all the insertion stages are minimized. R. Jackson *et al.* [19] developed a path planning method for autonomous robotic surgical suturing. Their method is mainly based on the best practices of manual suturing from surgeons.

In this paper, we propose a novel layout optimization method for the robot-assisted surgery system and navigation camera in the OR. The surgical robot is positioned to reach all target points, and the optical tracking camera should continuously track the tracking markers attached to the patient and the robot. Moreover, path planning optimization for robot motion have been addressed to reduce the workspace and the operation time.

## 2. METHODS

### 2.1. Problem definition

The conventional OR layout, as shown in Fig. 1, includes C-arm X-ray system, patient bed, surgeons, surgical robot, and optical tracking camera. As an example operation, we applied the proposed method to robot-assisted anterior cruciate ligament (ACL) reconstruction surgery [20]. In robot-assisted ACL reconstruction, the main surgical systems are a surgical robot and an optical tracking camera. The surgical robot locates the end-effector to accurately make preoperatively planned tunnels, while the optical tracking camera system tracks the markers attached to the patient and the robot and determines the relative coordinates of the patient and the robot. The patient bed, the surgical robot, and the optical camera in a simple OR layout are illustrated in Fig. 2. The end-effector of the robot, the robot base, and the camera are defined in a coordinate system fixed at  $O_o$  and transformed by the matrix  ${}^o_eT$ ,  ${}^o_rT$  and  ${}^o_cT$ , respectively. The end-effector's transformation matrices with respect to the robot base and the camera coordinate system are computed as follows:

$${}^r_eT = {}^r_oT^{-1} \cdot {}^o_eT, \quad (1)$$

$${}^c_eT = {}^c_oT^{-1} \cdot {}^o_eT, \quad (2)$$

where  ${}^r_eT$ ,  ${}^c_eT$  is the transformation matrix of the end-effector with respect to the robot base and camera coordinate, respectively. The matrix  ${}^o_rT$  includes position ( $p_x$ ,  $p_y$ ,  $p_z$ ) and orientation ( $r_x$ ,  $r_y$ ,  $r_z$ ) of the robot base; the matrix  ${}^o_cT$  includes position ( $c_x$ ,  $c_y$ ,  $c_z$ ) and orientation ( $r_{cx}$ ,  $r_{cy}$ ,  $r_{cz}$ ) of the optical camera. From (1), and (2) the unknown variables  ${}^r_oT$  and  ${}^c_oT$  should be determined for robot and optical camera placement.

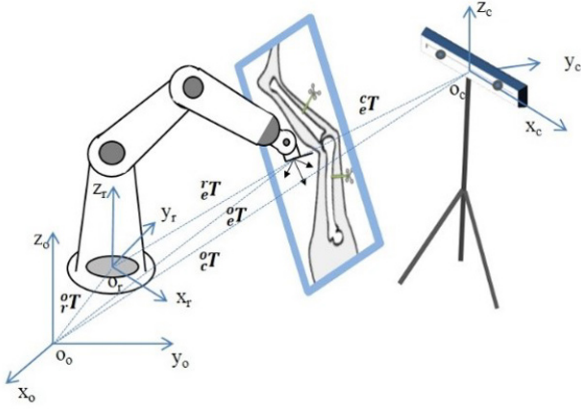


Fig. 2. Coordinate system of the robot and optical camera.

Because both the robot and camera are coplanar and are placed on the ground, we have  $\{p_z, r_x, r_y, r_{cy}\} = 0$ . The unknown variables are  $\{p_x, p_y, r_z\}$  for the robot positioning and  $\{c_x, c_y, c_z, r_{cx}, r_{cz}\}$  for the camera positioning. The end-effector of the surgical robot is designed as a straight line as shown in Fig. 3.

### 2.1.1 Kinematics criteria

Several kinematic performance criteria have been proposed by Zeghloul and Pamana [21] for optimal placement of robotic manipulator. However, for robotic-assisted surgery where the end-effector must reach to some surgical points and can pass close to a singular position which results in excessive joint velocities and torques. To prevent this problem, it is necessary to use the manipulability measure as a kinematic criteria for the optimal placement. The manipulability measure introduced by Yoshikawa is

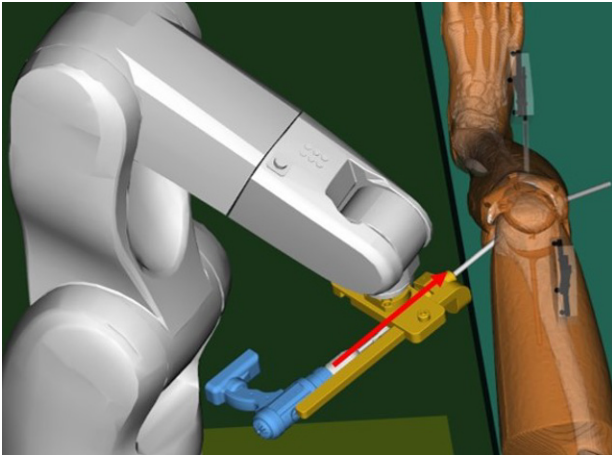


Fig. 3. Simulated surgical robot for ACL reconstruction. The red arrow indicates the robot end-effector to make surgical tunnels.

expressed by the following index Yoshikawa [22]:

$$w = \sqrt{\det(J \cdot J^T)}, \quad (3)$$

where  $J$  is Jacobian matrix of robot, computed from the kinematics description of robot.

### 2.1.2 Optical constraint

During the robotic-assisted surgery, using optical tracking, the tracking markers attached to the robot and patient should be tracked continuously by the optical camera. Thus, the optical constraint of the marker's visibility is determined by the following index:

$$f_{mv} = \begin{cases} 1 & (M_i \cap FOV) = 1 \\ 0 & \text{Otherwise,} \end{cases} \quad (4)$$

where  $M_i$  is the marker attached to the patient and robot and  $FOV$  is the field of view of the optical tracking camera.

## 2.2. Genetic algorithms (GA)

In conventional methods for optimization problems, a precise mathematical model is always required. For example, Gradient Descent is a classical numerical optimization method used to find the local optimum by searching from a single point [23]. When implementing a practical algorithm, especially for multi degree of freedom of robot system, any changing of model of the manipulator, the formulation of the optimization needs change accordingly. Moreover, Gradient Descent do not find the global optimum, so the optimal result is not the best optimal results, so the motion of robot easily occurs on singular point which is unwanted case. Therefore, an intelligent optimization method known as a Genetic algorithm (GA) is proposed to find the optimal base placement of the robot.

The GA is a well-known efficient global optimization algorithm was introduced by Holland [24] that uses the concept of biological structure to natural selection and survival of the fittest. Unlike Gradient Descent method, GA can be used when no information is available about the gradient of the function at the evaluated points. GA can still achieve good results even in cases in which the function has several local minima or maxima. The principle of the GA combines a number of ranking, *selection* techniques, *mutation*, and *crossover* to perform on the exploited *chromosomes* to produce the exploration set for the next generation. The parameters involved in the GA procedure are selected as follows: we encode the position and orientation of the robot base and the camera base into chromosomes. The chromosomes is comprised four genes (for robot base) and five genes (for camera base). Because they are real values, so decimal encoding was preferred to

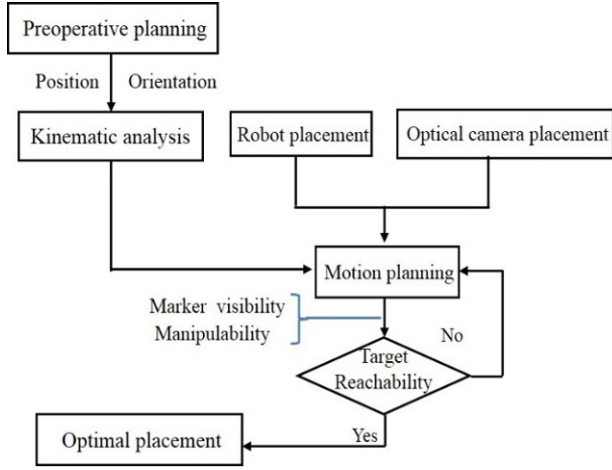


Fig. 4. Flowchart diagram of the optimization process.

binary. The initial population of individuals= 50, selection is tournament, crossover is single point, and mutation probability= 0.8.

### 2.3. Layout optimization

The sequences to perform the optimization of surgical robotic system positioning are illustrated in Fig. 4. As shown in Fig. 5, the position and orientation of the femoral and tibial tunnels are defined in preoperative planning step for ACL reconstruction [25]. By analyzing and solving the inverse kinematics of the robot using Denavit-Hartenburg (D-H) parameters in Fig. 6 and the closed-form solution Craig [26], the joint angle values are found for end-effector pose. In the first loop, for the initial positions of the robot and camera, motion planning of the robot is implemented with marker visibility and manipulability constraints. If the robot can reach the target point while the optical camera continuously tracks the marker, the positions of the robot base and camera base are the optimal positions. Otherwise, new positions of the robot and camera are found through the optimization process. To define the objective function, we applied kinematics criteria from (3) and the optical constraints for robot and optical camera placement from (4), respectively.

For robot base placement, the objective function is the sum of inversed manipulability measures and can be described by the following expression:

$$F_1 = \sum_{k=1}^n \frac{1}{w_k}, \quad (5)$$

where  $n$  is the number of prescribed poses and  $w_k$  is the manipulability measure for a robot configuration of pose  $k$ . Hence, our research's object is described in Fig.4, so there are two poses for robot end-effector (the first and the second surgical target point,  $n = 2$ ).

For camera base placement, there are five parameters including 3 parameters for position and 2 parameter for

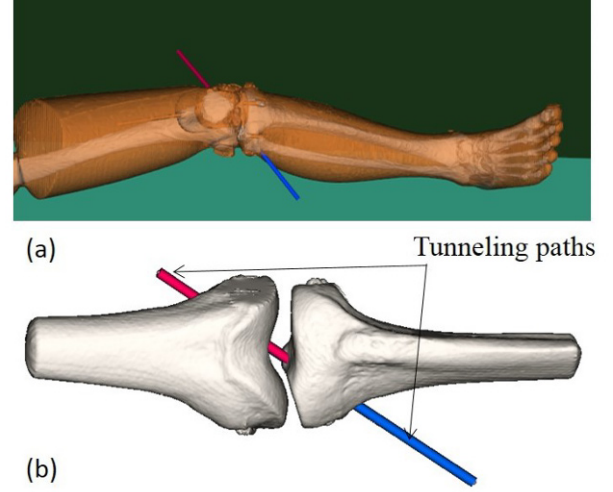


Fig. 5. (a) Preoperatively planned position and orientation of tunneling paths for anterior cruciate ligament (ACL) reconstruction surgery and (b) the detailed view of tunneling paths with bone models.

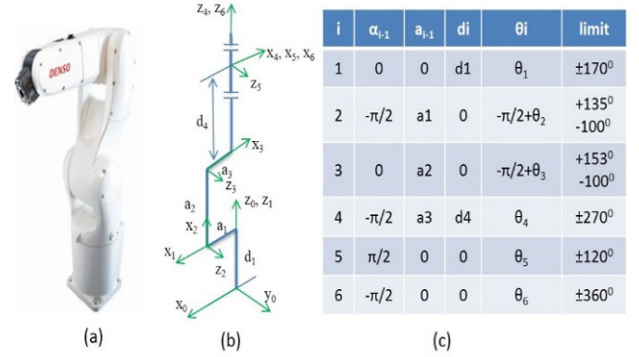


Fig. 6. (a) Six-axis robot arm used in the experiment; (b) Kinematics model of the robot arm; (c) Denavit-Hartenburg (D-H) parameters.

title angle and they are independent of each other. Therefore, the objective function can be defined in (6) and (7) for camera's position and title angle, respectively.

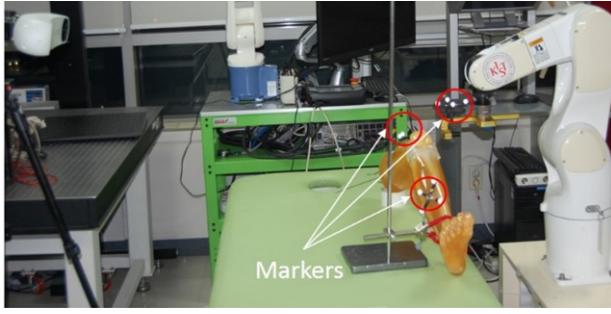
$$F_2 = \sum_{i=1}^m \sqrt{(x - x_i)^2 + (y - y_i)^2 + (z - z_i)^2}, \quad (6)$$

$$F_3 = \sum_{i=1}^m \sqrt{(\theta_x - \theta_{xi})^2} + \sqrt{(\theta_z - \theta_{zi})^2}, \quad (7)$$

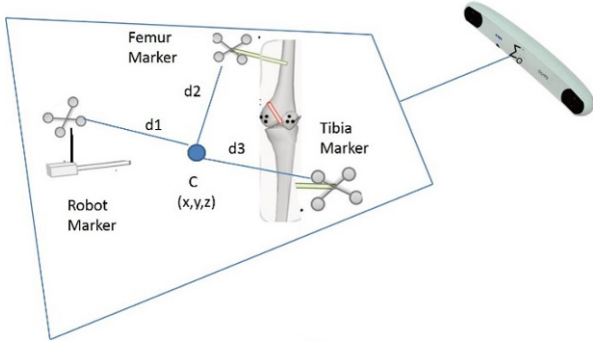
where  $x_i$ ,  $y_i$ , and  $z_i$  are coordinates of the makers in 3D space and  $\theta_{xi}$  and  $\theta_{zi}$  are the rotation of the markers around the  $x$  and  $z$  axes.

For markers attached to the phantom as shown in Fig. 7(a),  $F_2$  is the sum of the distance from the center of the FOV of the optical tracking camera to the center of the markers and  $F_3$  is the sum of the deviations of markers' normal angles around the  $x$  and  $z$  axes (Fig. 7(b)).





(a)



(b)

Fig. 7. (a) Markers attached to the phantom and robot, (b) configuration of the markers with respect to camera's field of view (FOV).

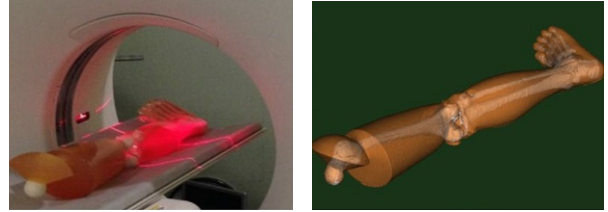
By minimizing the objective function  $F_1$ ,  $F_2$  and  $F_3$ , the optimal values of the unknown parameters are determined. During the optimization procedure, the imposed constraints regarding the unknown variables are described by

$$x_{l\min} \leq x_l \leq x_{l\max}, \quad (8)$$

where  $l = 1, 2, \dots, m$  and  $m$  is the number of variables. Constraint (8) takes into account the limits of the geometry of the robot base and the camera position in the OR layout.

#### 2.4. Path planning optimization

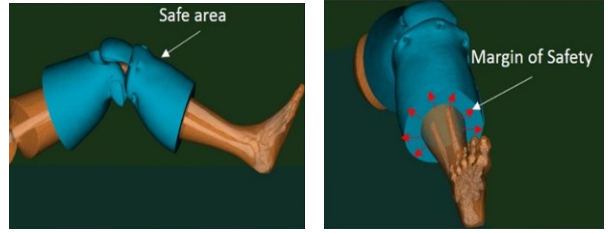
In the OR, the workspace of robot is often limited by avoiding collision with surrounding objects. Therefore, it is necessary to optimize the path of robot end-effector when moving to the surgical target. Hence, the path end-effector to reach the surgical target and move between the surgical targets (Fig. 5) needs to be carefully planned through a predefined curve. Unlike the previous researches, we propose a path planning method mainly based on 3D geometry of surgical object (patient's leg in our application case). Firstly, we design a 3D virtual model of the patient's leg based on a phantom lower limb. To create the 3D virtual model, we took CT scanning of



(a)

(b)

Fig. 8. (a) Leg phantom is taking CT scan and (b) 3D virtual leg model.



(a)

(b)

Fig. 9. (a) Safe area of leg's 3D virtual model and (b) Margin of safety.

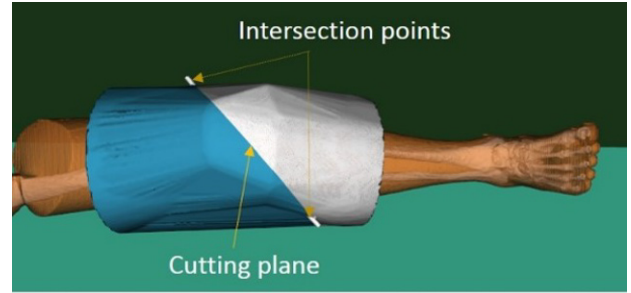


Fig. 10. Cutting plane through two intersection points.

the phantom model as illustrated in Fig. 8(a). Next, 3D geometrical models of leg were prepared and visualized by using Visualization Tool Kit (VTK) [27] as shown in Fig. 8(b).

Then, safe area is created by boolean operation from 3D virtual models as shown in Fig. 9(a). The margin of safety is illustrated in Fig. 9(b) is selected so that patient does not collide with the robot end-effector when considering to track the patient movement. After defining safe area, we create a cutting plane through two intersection points as show in Fig. 10. The first and second intersection points are found by intersecting the safe area and the surgical targets (femoral and tibia tunnels).

#### 2.5. Validation test

We validated the layout optimization and path planning optimization results of the proposed methods. We implemented the experimental tests as an exemplar OR layout with a robotic system (VS068, Denso, Japan [28]) with an



Fig. 11. Experimental layout of operating room to validate the proposed methods.

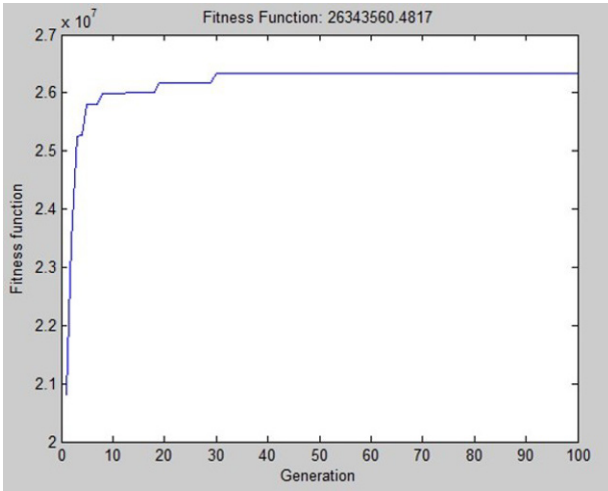


Fig. 12. Fitness function value changes during the optimization by using genetic algorithm (GA).

optical tracking camera (NDI, Canada [29]) and a phantom lower limb (Kyoto Kagaku, Japan [30]) as shown in Fig. 11.

### 3. RESULTS AND DISCUSSION

The geometric bounds of the variables of the validation test are presented in Table 1. In the first loop of the GA, initial populations are randomly formed to set variable values, which are used to calculate the objective function value. When the maximum number of generations is achieved, the variable values corresponding to the minimum fitness values are selected as given in Table 2.

Fig. 12 shows the fitness function values versus the generation number. As shown in Fig. 11, from the first generation to the 30th generation, the fitness function values continuously increase; however, after the 30th generation, the fitness function becomes almost unchanged after convergence. To validate the correlation between the actual



(a)



(b)

Fig. 13. Checking the reachability for (a) the first surgical target; and (b) the second surgical target.

experimental results in Fig. 11 and the simulation results in Fig. 12, we implemented the reachability testing of the surgical targets (the femoral tunnel and tibial tunnels) as shown in Fig. 13. The visibility of the optical markers was also checked by the obtained optimal position of the camera. As a result, the surgical robot could reach all target points and the optical camera could continuously track the markers attached to both the patient and the robot. The experiment proved that the suggested layout facilitates proper placement for the robot and the camera.

For the repeatability test, eight different initial positions of the robot base were randomly experimented with Fig. 14(a). As shown in Fig. 14(b), the optimal coordinates of the robot base become similar after the optimization process. The average deviations of all the optimal positions of the eight cases are 1.4 and 4.2 mm for x and y coordinates, respectively. The repeatability results show that the optimal position is nearly the same despite different initial positions.

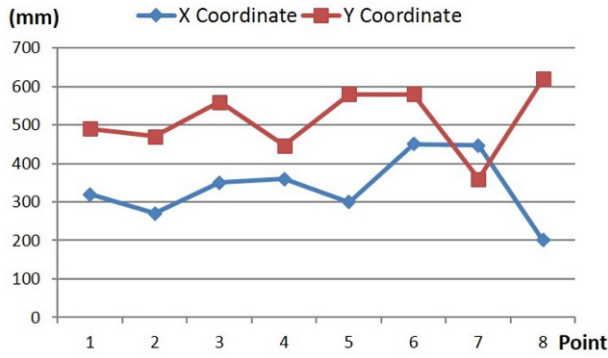
Table 3 gives the reachability test results of the robot end-effector with eight different initial positions. For example, from initial positions (1, 3, 7, 8), the robot end-

**Table 1.** Geometric bounds of unknown variables of the validation test.

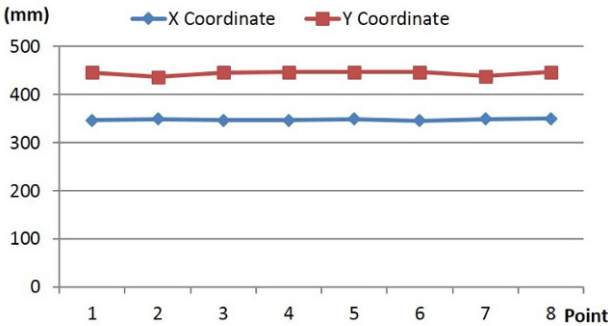
Variables	$p_x$ (mm)	$p_y$ (mm)	$r_z$ ( $^\circ$ )	$c_x$ (mm)	$c_y$ (mm)	$c_z$ (mm)	$r_{cx}$ ( $^\circ$ )	$r_{cz}$ ( $^\circ$ )
Min	200	200	0	500	2000	1000	0	0
Max	600	650	90	2000	3200	1500	90	90

**Table 2.** Optimized positional variables for robot base position and camera base position and its title angle.

Variables	$p_x$ (mm)	$p_y$ (mm)	$r_z$ ( $^\circ$ )	$c_x$ (mm)	$c_y$ (mm)	$c_z$ (mm)	$r_{cx}$ ( $^\circ$ )	$r_{cz}$ ( $^\circ$ )
Value	394	595	88	650	2420	1320	20	15



(a)



(b)

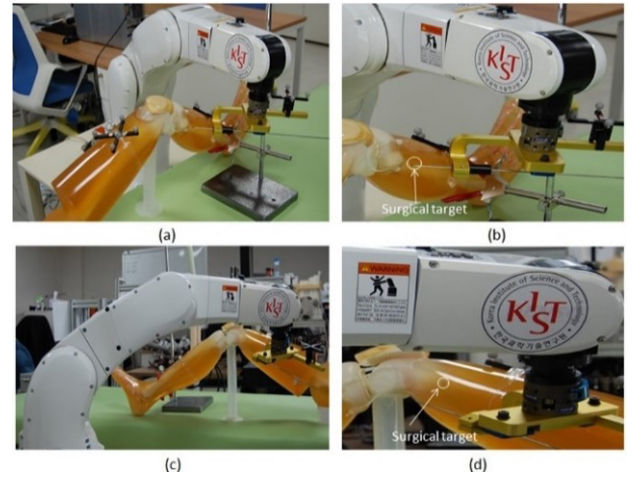
**Fig. 14.** The repeatability tests of the proposed method. (a) The change of initial coordinates and (b) optimal coordinates of the robot base.

effector could only reach the second surgical target (Fig. 15(a) and 15(b)), but it could not reach the first surgical target because the target was located out of the robot's workspace (Fig. 15(c) and 15(d)). In contrast, from initial points (2, 4, 6), the robot end-effector could reach only the first surgical target. Both the first and second surgical targets could only be reached from initial points (4, 7) while neither surgical target could be reached from position 5. In comparison with the traditional method of finding the suitable initial point, our proposed method could automatically find the optimal initial position from where the robot end-effector could reach all surgical targets.

After calculating the path planning by the proposed

**Table 3.** Reachability test results with eight different initial positions (O: reachable;  $\times$ : unreachable).

Initial position	1	2	3	4	5	6	7	8
1st surgical target	$\times$	O	$\times$	O	$\times$	O	O	$\times$
2nd surgical target	O	$\times$	O	O	$\times$	$\times$	O	O

**Fig. 15.** Reachability test results: (a) an example case where the surgical target could be reached and (b) its detailed view; (c) an example case where the surgical target could not be reached and (d) its detailed view.

method as shown in Fig. 10, the boundary line is extracted as shown in Fig. 16(a). The extracted boundary line is used as the trajectory for robot end-effector movement from the first surgical point to the second surgical point as shown in Fig. 16(b). When robot positioning parameter and camera positioning parameter are achieved as in Table 2, we validated path planning by 3D virtual simulation. The sequence of the motion of the surgical robot to perform the planned task is presented in Fig. 17. Firstly, the robot reaches the first surgical target (femoral tunnel). Next, the robot moves to the second surgical target (tibial tunnel) through the planned trajectory calculated by the proposed method. The results showed that the proposed



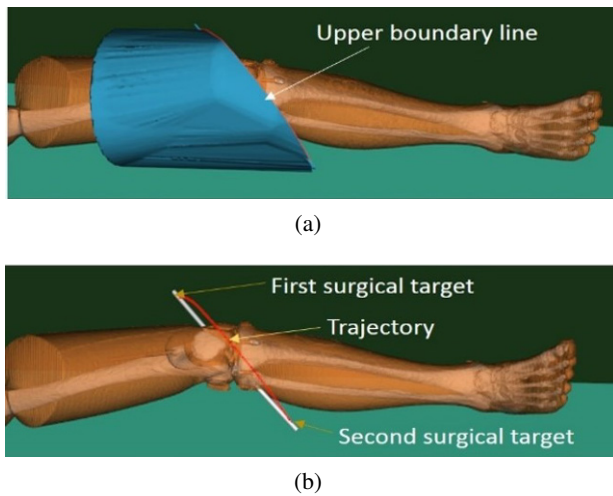


Fig. 16. (a) Extracting the boundary line from cutting plane and (b) calculated trajectory based on the proposed method.

method could successfully suggest a proper planning path from the first target to the second surgical target.

#### 4. CONCLUSION

Optimization of the OR layout was presented using kinematics criteria combined with optical constraints and genetic algorithms. Simulation and experimental results verified that the layout optimization could solve the target reachability problem. The proposed method can effectively decrease the preparation time required for robot-assisted surgery by avoiding repositioning of the system. In addition, the cutting plane method based on 3D geometry of the surgical object is developed and is successfully verified for path planning of surgical robot motion. In this study, the optimization of the OR layout and path planning for robotic surgery were attempted for the first time and we plan to apply the proposed method to clinical use in future experiments. In addition, we are considering the application of robot-path calculation to update the planned path when the patient moves during surgery.

#### REFERENCES

- [1] E. F. Correa and M. S. Dutra, "Manipulator Base Placement solved with Heuristic Search," *ABCm Symposium Series in Mechatronics*, vol. 6, pp. 896-905, 2014.
- [2] B. Kamrani, V. Berbyyuk, D. Wapling, S. Uwe, and X. Feng, "Optimal robot placement using response surface method," *Int'l Journal Advanced Manufacturing Technology*, vol. 44, no. 1, pp. 201-210, 2009.
- [3] K. A. Malek and W. Yu, "On the placement of serial manipulator," *Proceedings of DET C00 2000 ASME Design Engineering Technical Conference*, Maryland, pp. 1-8, 2000.
- [4] G. He, H. Gao, G. Zhang, and L. Wu, "Using adaptive genetic algorithm to the placement of serial robot manipulator," *Proceedings of the IEEE Int'l Conference on Engineering of Intelligent System*, pp. 1-6, 2006.
- [5] L. Tian and C. Collins, "Optimal placement of a two-link planar manipulator using a genetic algorithm," *Robotica*, vol. 23, no. 2, pp. 169-176, 2005. [click]
- [6] S. Mitsi, K. D. Bouzakis, D. Sagris, and G. Mansour, "Determination of optimum robot base location considering discrete end-effector positions by means of hybrid genetic algorithm," *Robotics and Computer- Integrated Manufacturing*, vol. 24, no. 1, pp. 50-9, 2008.
- [7] G. C. Vosniakos and E. Matsas, "Improving feasibility of robotic milling through robot placement optimisation," *The Journal Robotics and Computer-Integrated Manufacturing*, vol. 26, no. 5, pp. 517-525, 2010. [click]
- [8] J. Yang, W. Yu, J. Kim, and K. Malek, "On the placement of open-loop robotic manipulators for reachability," *Mechanism and Machine Theory*, vol. 44, no. 4, pp. 671-684, 2009. [click]
- [9] M. B. Trabia and M. Kathari, "Placement of a manipulator for minimum cycle time," *Journal of Robotic Systems*, vol. 16, no. 8, pp. 419-431, 1999.
- [10] R. D. Santos, V. Steffen, and S. Saramago, "Optimal task placement of a serial robot manipulator for manipulability and mechanical power optimization," *Intelligent Information Management*, vol. 2, no. 9, pp. 512-525, 2010. [click]
- [11] L. Adhami and E. V. Maniere, "Positioning tele-operated surgical robots for collision-free optimal operation," *Proceedings of the 2002 IEEE Int'l Conference on Robotics and Automation*, Washington, DC, pp. 2962-2967, 2002.
- [12] L. Adhami and E. V. Maniere, "Optimal planning for minimally invasive surgical robots," *IEEE Transactions on Robotics and Automation*, vol. 19, no. 5, pp. 854-863, 2003.
- [13] E. V. Maniere, L. Adhami, F. Mourgues, and A. Carpentier, "Planning, simulation, and augmented reality for robotic cardiac procedures: the STARS system of the ChiR team," *Seminars in Thoracic and Cardiovascular Surgery*, vol. 15, no. 2, pp. 141-156, 2003. [click]
- [14] J. G. Barbosa, T. G. Ramiirez, J. Salas, J. B. H. Ramos, and J. R. Jimenez, "Optimal Camera Placement for Total Coverage," *Proceedings of the IEEE Int'l Conference on Robotics and Automation*, pp. 844-848, 2009.
- [15] K. Yabuta and H. Kitazawa, "Optimum Camera Placement Considering Camera Specification for Security Monitoring," *Proceedings of the IEEE Int'l Conference on Circuits and System*, pp. 2114-2117, 2008.
- [16] E. Yildiz, K. Akkaya, E. Sisikogle, and M. Y. Sir, "Optimal camera placement for providing angular coverage in wireless video sensor networks," *IEEE Transactions on Computers*, vol. 63, no. 7, pp. 1812-1825, 2014.
- [17] R. Ye and Y. Chen, "Path planning for robot assisted femur shaft fracture reduction: a preliminary investigation," *Proc. of Int'l Conference on Virtual Environments, Human-Computer Interfaces and Measurements System*, Hong Kong, China, pp. 113-117, 2009.



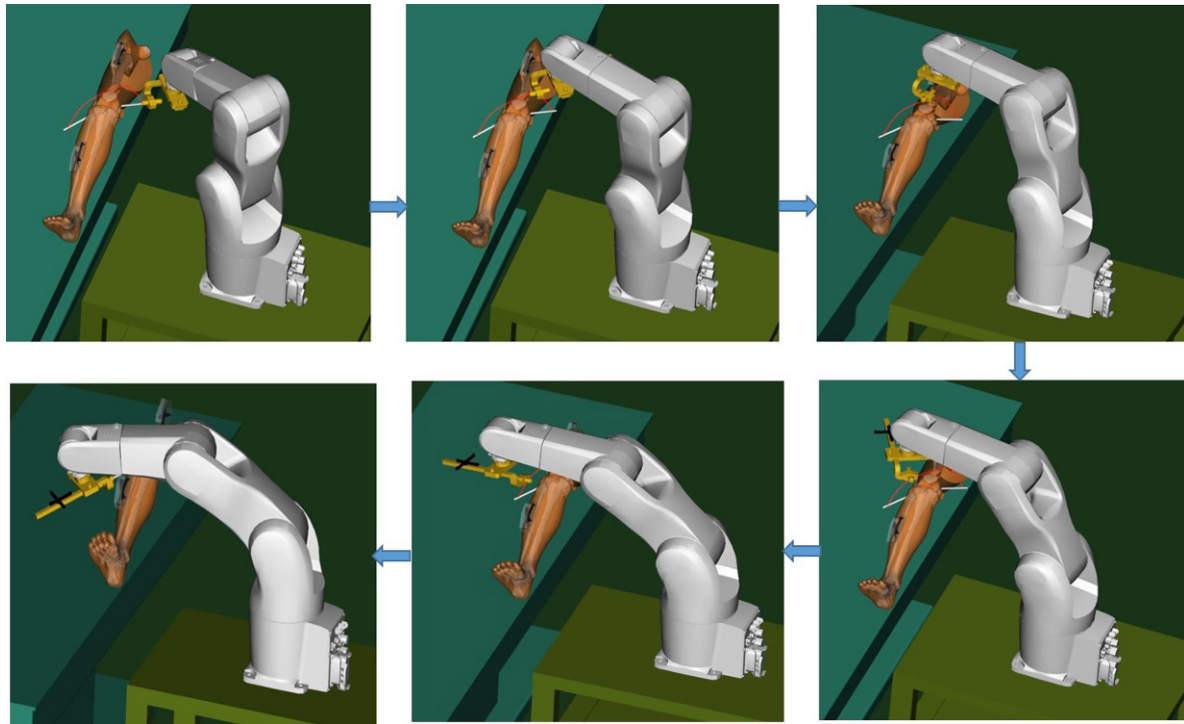


Fig. 17. Surgical robot movement along the planned path from the first surgical target to the second surgical target.

- [18] J. Zhang, J. Roland, S. Manolidis, and N. Simaan, "Optimal path planning for robotic insertion of steerable electrode arrays in cochlear implant surgery," *Journal of Medical Devices*, vol. 3, no. 1, pp. 11001-11010, 2008. [click]
- [19] R. C. Jackson and M. C. Cavusoglu, "Needle path planning for autonomous robotic surgical suturing," *Proceedings of the IEEE Int'l Conference on Robotics and Automation*, pp. 1669-1675, 2013.
- [20] S. Lim, J. Choi, Y. Kim, D. Lee, S. Park, and J. Wang, "Robotic guide system for reducing human alignment error in computer-assisted anterior cruciate ligament reconstruction," *Int'l Journal of Computer Assisted radiology and Surgery 2014*, vol. 9, no. 1, pp. 152-153, 2014.
- [21] S. Zeghloul and J. A. Pamames, "Multi-criteria optimal placement of robots in constrained environment," *Robotica*, vol. 11, no. 2, pp. 105-110, 1993. [click]
- [22] T. Yoshikawa, "Manipulability of robotic mechanisms," *The International Journal of Robotics and Research*, vol. 4, no. 2, pp. 3-9, 1985.
- [23] C. Bishop, *Pattern Recognition and Machine Learning*, Springer, New York, USA, 2006.
- [24] J. H. Holland, *Adaption in Natural and Artificial System*, University of Michigan Press, Ann Arbor, 1975.
- [25] J. Choi, S. Lim, Y. Kim, D. Lee, and S. Park, "3D pre-operative surgical planning software for anterior cruciate ligament reconstruction," *Proc. of 13th Int'l Conference on Control, Automation and Systems*, Gwangju, Korea, pp. 344-346, 2013.
- [26] J.J. Craig, *Introduction to Robotics: Mechanics and Control*, Prentice Hall Publishing Company, New York, USA, 1989.
- [27] Kitware Inc., <http://www.vtk.org/>
- [28] Denso Wave Inc., <http://www.denso-wave.com/>
- [29] Northern Digital Inc., <http://www.ndigital.com/>
- [30] Kyoto Kagaku Inc., <http://www.kyotokagaku.com/>



computer vision.

**Quoc Cuong Nguyen** is a Ph.D. student in the Graduate School of NID Fusion Technology at Seoul National University of Science and Technology, Korea. He received his BS (2004) and MS (2008) in the Faculty of Mechanical Engineering at Ho Chi Minh City University of Technology, Vietnam. His research focuses on robotics, mechanism simulation, mechatronics, and



interests include 3D medical imaging software, medical simulation, and computer aided surgery.

**Youngjun Kim** is a senior researcher in the Center for Bionics at Korea Institute of Science Technology. He received his BS (2001), MS (2003), and Ph.D. (2009) in the School of Mechanical and Aerospace Engineering at Seoul National University. He researched in the Department of Radiation Oncology at Stanford University as a postdoctoral scholar (2013). His research



**HyukDong Kwon** is an associate professor at Seoul National University of Science and Technology. He received his BS (1983) and MS (1985) in the School of Mechanical and Aerospace Engineering at Seoul National University, and Ph.D. (1996) in the Department of Mechanical Engineering at University of Manchester.

He served for the Ministry of Science and Technology as Director in R&D Coordination and Budget (2008). He worked for Korea Institute for Industrial Technology as Senior Researcher (2002). His research interests include manufacturing measurement, computer integrated manufacturing, and ST policy.